Probing the mechanical properties of graphene using a corrugated elastic substrate

Scott Scharfenberg,[1] D. Z. Rocklin,[1,2] Cesar Chialvo,[1] Richard L. Weaver,[1,2] Paul M. Goldbart,[1,2] and Nadya Mason[1]

[1)] *Department of Physics, University of Illinois at Urbana-Champaign, 1110 West Green Street, Urbana, Illinois 61801*

[2)] *Institute for Condensed Matter Theory, University of Illinois at Urbana-Champaign, 1110 West Green Street, Urbana, Illinois 61801*

(Dated: 14 January 2011)

We examine the mechanical properties of graphene samples of thickness ranging from 1 to 17 atomic layers, placed on a micro-scale-corrugated elastic substrate. Using atomic force microscopy, we show that the graphene adheres to the substrate surface, and can substantially deform the substrate, with larger graphene thicknesses creating greater deformations. We use linear elasticity theory to model the deformations of the composite graphene-substrate system. We compare experiment and theory, and thereby extract information about graphene's bending rigidity, adhesion, critical stress for interlayer sliding, and sample-dependent tension.

The exceptional mechanical properties of graphene have made it attractive for nano-mechanical devices and functional composite materials[1]. Two key aspects of graphene's mechanical behavior are its elastic and adhesive properties. The elastic properties have been measured using nano-indentation[2] and pressurization[3] techniques, and the Young's modulus E was found to be exceptionally high, $\sim 1\,\mathrm{TPa}$. Graphene's van der Waals adhesion to surfaces has been examined theoretically[4], and local adhesion to nanoparticles has been studied[5]. However, it is typically difficult to extract experimental parameters for adhesion, despite the fact that graphene's adhesive properties can strongly influence its electronic and mechanical behavior. The dopant distribution and carrier mobility of a graphene layer can be significantly altered upon adhesion of the layer to a substrate[6,7]. Even suspended graphene is known to adhere to sidewalls, which introduces strain and modifies mechanical behavior[8,9]. In addition, the mechanical interplay between graphene and other materials has not been well studied, although it is crucial to the use of graphene in composite[1], flexible[10], or strain-engineered[11] materials.

In this Letter, we explore both elasticity and adhesion, which are evident in the interaction between micro-scale-corrugated elastic substrates and graphene samples of thicknesses ranging from 1 to 17 atomic layers. By using an atomic force microscope (AFM) to determine surface adhesion and deformations, we find that few layer graphene (FLG) can fully adhere to the corrugated substrate, and that thicker samples flatten the corrugated substrate more than thinner samples do. By developing a simple linear elasticity theory to model the flattening and adhesion as a function of layer thickness, we are able to extract information about various fundamental and sample-dependent properties, such as graphene's bending rigidity, adhesion, critical stress for interlayer sliding, and sample-dependent tension.

Sample substrates were prepared by casting a 3 mm thick layer of polydimethylsiloxane (PDMS)—which cures into a flexible, rubbery material—onto the exposed, corrugated surface of a writable compact disc. This resulted in approximately sinusoidal corrugations on the PDMS, having a wavelength of $1.5\,\mu\mathrm{m}$ and a depth of $200\,\mathrm{nm}$ (see Fig. 1a). Graphene was then deposited onto the PDMS via mechanical exfoliation[12]. Candidate samples were first located using optical microscopy, then imaged on an Asylum Research MFP-3D AFM. Figure 1a shows a topographic image of FLG on the PDMS; it is evident from the image that the graphene conforms to the corrugations, as illustrated in Fig. 1b.

In order to fit the experimental data to a theoretical model, it was necessary to determine (1) the thickness of the FLG, (2) the adhesion between the FLG and the PDMS, and (3) the height profile of the PDMS-FLG system. The soft, non-standard substrate created difficulty in measuring FLG thickness via established AFM and Raman techniques. Thus, the thickness was determined by using the AFM (in contact mode) to fold the flake onto itself, and then using the AFM again to measure the resultant FLG-FLG step height. An example of AFM-folded FLG is shown in Fig. 2a. The same flake could be folded at multiple locations to increase accuracy (typical accuracy was 1-2 layers), although, because the method was destructive, it had to be undertaken once all other measurements were completed.

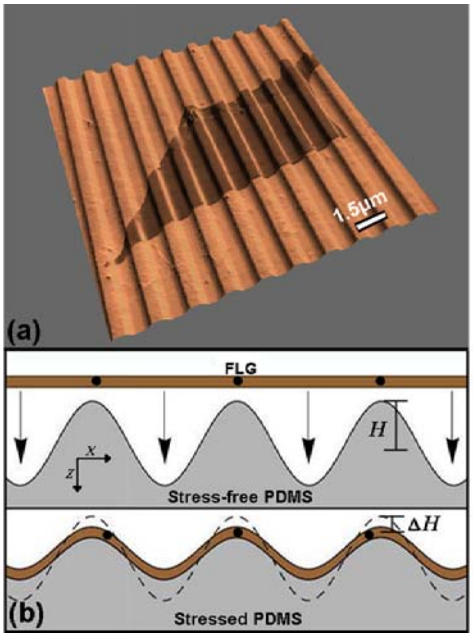

FIG. 1. **a.** AFM 3D topographic image of FLG on corrugated PDMS. AFM height and phase data are superimposed to create color contrast. **b.** Illustration of FLG-PDMS interaction, showing how FLG adheres to and flattens the PDMS corrugations. The coordinates and amplitudes relevant to the theoretical model are labeled.

The areas of the graphene that adhered to the PDMS were identified by measuring the phase of the oscillation of the AFM cantilever. This phase is determined by the electrostatic properties of the surface; in other words, sections having the same adhesion have common electrostatic properties and thus a common phase. The main image of Fig. 2b shows a two-dimensional phase map for 2-layer FLG, in which

the phase is uniform across the sample (except where adhesion is lost at the steepest slopes of the corrugation). These data demonstrate the near-conformal adhesion between the FLG and the PDMS, and are consistent with previous work on graphene placed over more shallow depressions[9]. The AFM height data similarly indicate that the FLG adheres to the corrugations of the PDMS (e.g., see Fig. 3). In contrast, the inset to Fig. 2b shows the phase data for 13-layer FLG, where bubble-like structure appears across the sample, showing that the phase is not uniform and, hence, that the FLG does not adhere well to the PDMS. In general, we found that samples having more than ~ 11 layers did not fully adhere; this is consistent with the predicted "snap-through" instability in graphene on a corrugated substrate[13]. The adhesive properties did not seem to depend on the size or aspect ratio of the graphene samples, only their thickness.

The most remarkable aspect of the FLG-PDMS system is that interplay between the rigidity of the graphene and the shear modulus of the PDMS causes the FLG to become corrugated and the PDMS to be flattened. Figures 3a and b show image and height measurements for 8- and 13-layer FLG on PDMS, respectively. In Fig. 3a it is clear that the FLG maintains the basic shape of the PDMS corrugations,

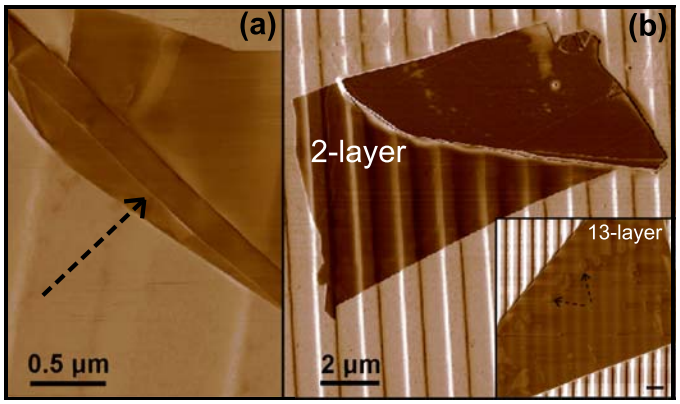

FIG. 2. **a.** Micrograph of FLG folded by AFM tip. FLG-FLG edges are used for thickness measurements. Dashed arrow points to fold and shows the direction in which AFM tip was dragged. **b.** AFM phase images of FLG on PDMS. Main figure: flake of FLG, where the lower-left section is 2-layer (upper right is much thicker, > 100 layers). The 2-layer region shows uniform adhesion over plateaus and valleys, indicated by homogeneous contrast over them. Adhesion loss, evident as bright and dark lines, occurs only at steepest regions between plateaus and valleys. Inset: 13-layer graphene showing inhomogeneous phase and adhesion; bubble-like lighter patches indicate where adhesion changes. Scale bar is $2\,\mu$m.

but pulls the corrugations up in the valleys and pushes them down on the plateaus. In contrast, Fig. 3b shows that 13-layer FLG sits on top of the PDMS; while the FLG likely strongly deforms the PDMS, the amount of flattening is difficult to determine because of the lack of adhesion. The 13-layer FLG is likely wavy due to slight sidewall adhesion, similar to what is seen in suspended graphene. Figure 4 shows the fractional height difference between the FLG-PDMS composite and the bare PDMS, plotted against graphene thickness, for 18 samples (measured on 9 different PDMS substrates); it is clear that the amount of flattening increases with layer number.

We now develop a linear elasticity theory, related to that of Yu and Suo[14], in which we determine the surface stress required on both the initially flat (ignoring the nanometer-scale intrinsic ripples) FLG and the initially corrugated PDMS, such that they each deform to accommodate the other. Continuum models have been applied previously to characterize the bending rigidity of few-layer graphene[16].

To start, we consider an undeformed PDMS substrate having a corrugated surface: $h(x) = H\cos kx$ (see Fig. 1b for coordinates). Height profiles that are not simple sine waves can be handled via the superposition of suitable terms. Graphene adheres to and flattens this surface, reducing the corrugation amplitude to $H - \Delta H$ (as discussed below). The normal stress $S\cos kx$ required to deform the graphene in this way then follows from thin plate theory[15], and is related to the deformed height profile via

$$M\nabla^4[(H - \Delta H)\cos kx] = S\cos kx, \tag{1}$$

where M is the flexural, or *bending*, rigidity of the FLG, so that $S = Mk^4(H - \Delta H)$. An equal

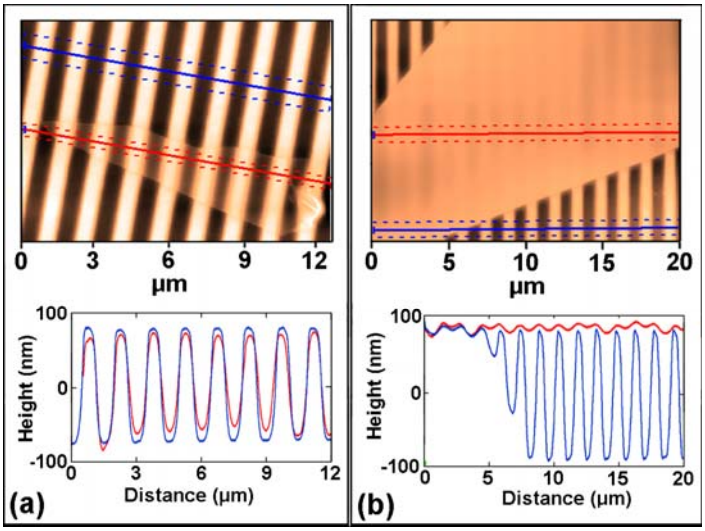

FIG. 3. Image (top) and height measurements (bottom) for **a.** 8-layer and **b.** 13-layer graphene. Red lines show trajectories of scans over graphene, corresponding to red height curves (averaged between the dotted lines). Blue lines show scans of surrounding PDMS substrate. Scans over PDMS alone are taken far from FLG, to provide a baseline height unaffected by FLG. Note the scale difference between vertical and horizontal axes in height vs. distance curves.

and opposite stress acts on the PDMS substrate, so we next determine how the PDMS responds to this stress.

We regard the PDMS as being a semi-infinite, isotropic, incompressible medium, and describe distortions of it by means of a displacement field $\vec{u}(x,z)$. (We only consider configurations that are translationally invariant in the y-direction, and hence are effectively two-dimensional.) At the linear level, to which we are working, incompressibility implies divergence-free displacements: $\vec{\nabla}\cdot\vec{u}=0$. The displacement $\vec{u}$ obeys the condition of mechanical equilibrium, i.e.,

$$\mu\nabla^2\vec{u}=\vec{\nabla}p, \tag{2}$$

in which μ is the shear modulus and p the pressure field, introduced to implement incompressibility, which requires that $\nabla^2 p=0$. In determining $\vec{u}$, the appropriate boundary condition involves specifying the normal component of the stress, which amounts to the condition (summing over repeated indices)

$$\mu\, n_i\left(\partial_i u_j\left(\vec{r}\right)+\partial_j u_i\left(\vec{r}\right)\right)-n_j\, p\left(\vec{r}\right)=f_j\left(\vec{r}\right), \tag{3}$$

in which $\vec{f}(\vec{r})$ is the external force acting on the PDMS at its surface and $\vec{n}(\vec{r})$ is the unit normal vector pointing outward from the PDMS surface. It is then straightforward to show that the PDMS responds by undergoing the position-dependent displacement

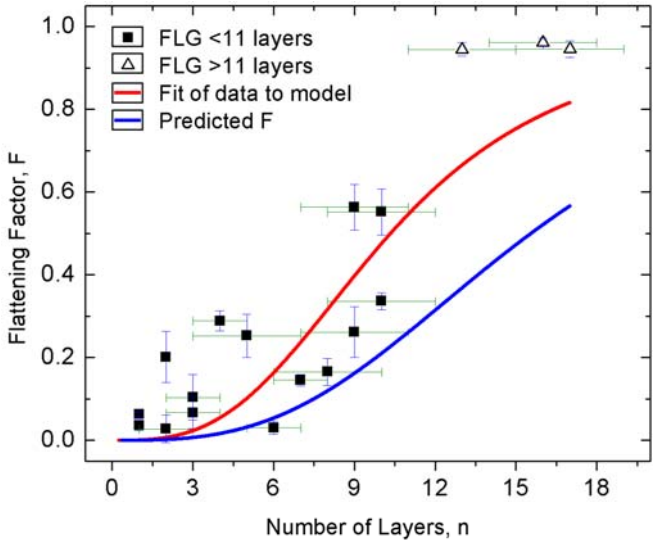

FIG. 4. Data and fits for flattening factor (fractional deformation of PDMS) vs. number of layers. Symbols show measured flattening for 18 FLG samples. Samples with thicknesses > 11 layers are shown with open triangles, as AFM height measurements are likely modified by the lack of adhesion to the substrate. A value of $F = 0$ corresponds to no flattening of the PDMS, whereas $F = 1$ corresponds to totally flattened PDMS. Error bars are related to the uncertainty in layer number and the spatial non-uniformity of flattening. Red curve is least squares fit to model, assuming zero tension in samples. Blue curve is predicted flattening for samples having zero tension (see text).

$$\begin{pmatrix} u_x \\ u_z \end{pmatrix} = -\frac{S}{2\mu k} \mathrm{e}^{-kz} \begin{pmatrix} kz\, \sin kx \\ (1+kz)\cos kx \end{pmatrix}. \tag{4}$$

In particular, the surface of the PDMS is displaced according to $(u_x, u_z)|_{z=0} = -(S/2\mu k)(0, \cos kx)$, which creates a surface profile $(H - \Delta H)\cos kx$. The amplitude is diminished from H by an amount

$$\Delta H = \frac{S}{2\mu k} = \frac{Mk^4(H - \Delta H)}{2\mu k}. \tag{5}$$

Rearranging gives the *flattening factor*

$$F \equiv \frac{\Delta H}{H} = \frac{(Mk^3/2\mu)}{1 + (Mk^3/2\mu)}. \tag{6}$$

We now compare the model to the data, to elucidate the FLG's mechanical behavior. Figure 4 shows measured values of F vs. n, along with a least squares fit to equation (6) (red curve) in which we assume M proportional to the cube of the number of layers, consistent with a continuum model for thick graphene[16] . From the fit we extract a dimensionless graphene rigidity parameter

$G \equiv Mk^3/2\mu n^3 = 0.00091$.

The shear modulus μ of PDMS was measured separately via nanoindentation and an ultrasonic probe, which gave $\mu = 0.4\,\mathrm{MPa}$ and $0.23\,\mathrm{MPa}$, respectively (the difference is possibly due to probing surface vs. bulk moduli). Using $\mu = 0.4\,\mathrm{MPa}$, as well as $k = 4.2\,\mu\mathrm{m}^{-1}$, the bending rigidity of n-layer FLG is then obtained as $M = 9.8{\times}10^{-18}n^3\,\mathrm{Nm}$. This value is higher than that predicted using Kirchhoff plate theory, from which $M = E\,(nt)^3\,/12\,(1-\nu^2) = 2.9{\times}10^{-18}n^3\,\mathrm{Nm}$, using the graphene Young's modulus $E \approx 900\,\mathrm{GPa}$[17], Poisson ratio $\nu \approx 0$, and per-layer thickness $t = 0.335\,\mathrm{nm}$[17]. The predicted values for F are plotted as the blue curve in Fig. 3.

The spread in the data is greater than can be accounted for by measurement uncertainty. This leads us to hypothesize that the discrepancy between extracted and predicted values of F (or M) is caused by tension in the graphene. Because of its high stiffness against stretching we believe the FLG slips along the pdms substrate as it is applied, until sample-dependent friction between the PDMS and the FLG is sufficient to halt the process, leaving some tension in the FLG (see dots in Fig 1). A tension T could modify the flattening factor in equation (6), giving

$$F \equiv \frac{\Delta H}{H_0} = \frac{(Mk^3/2\mu) + (Tk/2\mu)}{1 + (Mk^3/2\mu) + (Tk/2\mu)}. \tag{7}$$

If we assume that the difference between the predicted values of F (blue curve) and the data in Fig. 4 is due to tension, we can use equation (7) to extract a value of tension for each sample. This yields tension values between 0 and $0.20\,\mathrm{Nm}^{-1}$, with no discernible trend with thickness. The tension is positive for each sample, to within the margin of error, consistent with the picture that friction opposes the contraction of FLG as it conforms to the corrugated PDMS. The maximum tension corresponds to a maximum axial strain of $T/nhE = 7.8\times10^{-5}$. We can also use the tension to estimate the magnitude of the stress due friction: assuming the friction acts over a distance $d \geq 10\,\mu\mathrm{m}$, we find a stress T/d of less than $2{\times}10^4\,\mathrm{Pa}$. The condition that tension be positive, taken together with our data, implies that FLG's bending rigidity is no greater than $(1.6 \pm 0.8)n^3 \times 10^{-18}\,\mathrm{Nm}$, similar to predicted values. If, as seems reasonable, the tension is negligibly small for at least one sample, then this bound would become an estimate of the graphene rigidity.

The data shown in Fig. 4 can also be used to estimate the normal interface stress $S = 2\mu kFH$, which ranges from $(1.1 \text{ to } 3.0)\times10^5\,\mathrm{Pa}$. The data also show that no samples which adhere to the surface have $F > 0.6$, implying that the adhesive strength between the graphene and the PDMS is $\leq 3.0\times10^5\,\mathrm{Pa}$. Note that this stress is model-independent.

We can extract bounds on the graphene-PDMS adhesion energy by considering that the energy of the adhesion must be at least as large as the spatially-averaged elastic deformation energy. This energy can be regarded as a sum of contributions: the elastic deformation of the substrate $(1/2)\sigma_{ik}\big(u_{ik}-(p/\mu)\delta_{ik}\big) = S\Delta H\cos^2(kx)/2$; the FLG deformation under tension $(T/2)(Fh'(x))^2 = T(FH)^2k^2\cos^2(kx)/2$; and the FLG bending $(M/2)\big(Fh''(x)\big)^2 = M(FH)^2k^4\cos^2(kx)/2$[15]. Ignoring the negligible tension contribution,

the spatial average of these sums to $\mu k F H^2/2$. The maximum elastic energy (which is also the lower bound of the adhesive energy) in our samples is thus $0.044\,\mathrm{eV/nm^2}$. This is consistent with the theoretical prediction of $0.04\,\mathrm{eV/nm^2}$ for the van der Waals adhesive energy between graphene and a SiO_2 substrate[4]. Absent any other significant contributions to the energy budget (such as work done against friction), the adhesion energy must equal the elastic energy and $0.044\,\mathrm{eV/nm^2}$ becomes an estimate of the adhesive energy.

Even though thin plates have bending rigidity determined entirely by Young's modulus and thickness, there are nevertheless (small) shear strains developed interior to the plate (they are negligible in estimating bending rigidity.) There are in consequence shear stresses developed within the graphene slab that are opposed by interlayer shear strength. These stresses could cause the graphene layers to slide relative to one another. In this case, the impact on the flattening factor is to modify the dependence of the bending rigidity on the number of layers from n^3 for a cohesive sample to $\sum_a n_a^3$, where n_a is the number of layers in the a^{th} slab. We find that such a model does not improve the fits to the data, and thus find no evidence that the graphene layers slide. The physical effect of sliding would be to decrease the flattening factor, and thus sliding cannot explain the discrepancy between the theoretical values and data of Fig. 4. We hypothesize that there does, however, exist some critical shear stress beyond which layers slide relative to one another. Considering the finite thickness of the FLG, Mindlin plate theory[18] shows that the boundary stress needed to deform the FLG generates a central shear strain ϵ of

$$\epsilon = n^2 t^2 k^3 (H - \Delta H)/4. \tag{8}$$

The absence of evidence for sliding in samples of < 11 layers thus suggests a lower bound on the critical shear strain ϵ_{crit} of $\geq 1.2 \times 10^{-5}$. Multiplying by the graphene shear modulus, which we take to be half its Young's modulus, this implies a critical shear stress between the layers of $\geq 5.6\,\mathrm{MPa}$.

To conclude, we have developed a method of measuring the mechanical properties of graphene using deformable, micro-corrugated substrates. We are able to put bounds on—or extract estimates for—fundamental properties such as graphene's bending rigidity, critical shear stress, and the FLG-PDMS adhesive strength and energy. We also extracted sample-dependent properties such as the tension and normal interface stress. The experimental and theoretical techniques developed in this paper may be readily extended to various substrates having a range of surface geometries.

Acknowledgments. We thank Scott Maclaren (UIUC CMM) and Richard Nay (Hysitron) for technical assistance. This work was supported by DOE DE-FG02-07ER46453, NSF DMR06-44674, NSF DMR09-06780, and an NDSEG Fellowship (DZR).

REFERENCES

[1]See, e.g., A. K. Geim, *Science* **324**, 5934 (2009).

[2]C. Lee, X. Wei, J. W. Kysar, and J. Hone, *Science* **321**, 385 (2008).

[3]J. S. Bunch, S. S. Verbridge, J. S. Alden, A. M. V. D. Zande, J. M. Parpia, H. G. Craighead, and P. L. McEuen, *Nano Lett.* **8**, 2458 (2008).

[4]J. Sabio, C. Seoanez, S. Fratini, F. Guinea, A. H. Castro Neto, and F. Sols, *Phys. Rev. B* **77**, 195409 (2008).

[5]Z. Zong, C. Chen, M. R. Dokmeci, and K. Wan, *Jour. App. Phys.* **107**, 026104 (2010).

[6]X. Du, I. Skachko, A. Barker, and E. Y. Andrei, *Nature Nanotech.* **3**, 491 (2008).

[7]K. I. Bolotin, K. J. Sikes, J. Hone, H. L. Stormer, and P. Kim, *Phys. Rev. Lett.* **101**, 096802 (2008).

[8]J. S. Bunch, A. M. van der Zande, S. S. Verbridge, I. W. Frank, D. M. Tanenbaum, J. M. Parpia, H. G. Craighead, and P. L. McEuen, *Science* **315**, 490 (2007).

[9]C. Metzger, S. Remi, M. Liu, S. V. Kusminskiy, A. H. Castro Neto, A. K. Swan, and B. B. Goldberg, *Nano Lett.* **10**, 6 (2010).

[10]J.A. Rogers, T. Someya, and Y. Huang, *Science* **327**, 1603 (2010).

[11]F. Guinea, M. I. Katsnelson, and A. K. Geim, *Nature Physics* **6**, 30 (2010).

[12]K. S. Novoselov, A. K. Geim, S. V. Morozov, D. Jiang, Y. Zhang, S. V. Dubonos, I. V. Grigorieva, and A. A. Firsov, *Science* **306**, 666 (2004).

[13]T. Li, and Z. Zhang, *Nanoscale Res. Lett.* **5**, 169 (2010)

[14]H. H. Yu, and Z. Suo, *J. Mech. Phys. Solids* **46**, 5 (1998)

[15]See, e.g., L. D. Landau, and E. M. Lifshitz, *Theory of Elasticity* (Course of Theoretical Physics, Vol. 7) (Pergamon, Oxford, 1986), Sec. 11,12.

[16]M. Poot, and H. S. J. van der Zant, *Appl. Phys. Lett.* **92**, 063111 (2008).

[17]B. T. Kelly, *Physics of Graphite* (London: Applied Science, 1981).

[18]R. D. Mindlin. *Jour. Appl. Mech.* **18**, 31 (1951).